Journal of Materials Chemistry A

PAPER

View Article Online
View Journal | View Issue



Cite this: J. Mater. Chem. A, 2016, 4, 15240

# A bifunctional metal–organic framework featuring the combination of open metal sites and Lewis basic sites for selective gas adsorption and heterogeneous cascade catalysis†

Hongming He,[ab] Fuxing Sun,[a] Briana Aguila,[b] Jason A. Perman,[b] Shengqian Ma*[b] and Guangshan Zhu*[a]

Received 18th June 2016
Accepted 12th September 2016

DOI: 10.1039/c6ta05098k

www.rsc.org/MaterialsA

A bifunctional MOF (JUC-199) featuring dual functionality, open metal sites ($Zn^{2+}$) and Lewis basic sites ($-NH_2$), has been successfully synthesized using a custom-designed ligand. JUC-199 demonstrated good selective gas sorption behaviours with IAST selectivity values of 9, 30, 37 and 64 at 298 K and 101 kPa for $CO_2/CH_4$, $CO_2/N_2$, $C_2H_6/CH_4$ and $C_2H_4/CH_4$ respectively; surpassing those of most MOFs reported thus far. Moreover, JUC-199 can serve as a heterogeneous cascade catalyst to efficiently catalyse the tandem one-pot deacatalization-Knoevenagel condensation reaction.

## Introduction

Energy crises and environmental pollution represent some worldwide issues needing to be addressed with urgency. In particular, the escalating anthropogenic carbon dioxide ($CO_2$) emissions have drawn special attention from chemists and materials scientists in recent years because it is the primary source of greenhouse gases causing dire environmental concerns.[1–4] Among all the separation technologies, adsorption separation is one of the most promising approaches.[5–8] In addition, methane ($CH_4$), as the main component of natural gas and biogas, is a considerably cleaner energy source for our daily lives and a useful $C_1$ feedstock chemical to prepare various chemicals in the petrochemical industries, such as acetylene and chloromethane.[9,10] However, a small quantity of hydrocarbon impurities with methane will hinder its cleaner qualities over other fossil fuels. At the present, growing interest to develop porous materials that efficiently capture or separate post-combustion $CO_2$ or purify $CH_4$ from natural gas and biogas are desired.

Recently, there is an escalating interest in the development of one-pot, sequential and multi-capable reactions because of their comparably higher efficiency, less waste, lower cost and fewer purification steps.[11–13] These multi-step cascading reactions have spurred great attention in developing and exploration upcoming materials as catalysts. Nonetheless, it is usually very difficult to develop a catalyst requiring both acidic and basic components because these moieties can easily deactivate each other. Therefore, it remains a challenge to develop site-isolating and multifunctional heterogeneous catalysts that can promote one-pot sequential reactions.

Metal–organic frameworks (MOFs),[14–21] are a new class of porous crystalline materials that have attracted tremendous interest due to their strong application scope in catalysis,[22–24] gas separation and storage,[25–27] sensing,[28–32] drug delivery,[33–35] and optical devices.[36–38] Inspired by the investigations on MOFs, their structures and properties can be designed and tuned through the judicious combination of organic linkers molecules and metal-containing secondary building units (SBUs). Hence, we postulate that if the ligands containing Lewis basic sites (LBSs) and the SBUs possessing unsaturated open metal sites (OMSs) are utilized, it is anticipated to afford bifunctional MOFs that are capable of selectively adsorbing gas molecules and also serving as heterogeneous catalysts for acid–base one-pot reactions. Recently, much effort has been devoted to obtaining multifunctional MOFs for multi-disciplinary applications.[39] Pal and co-workers reported a copper MOF that exhibited gas sorption and catalytic abilities.[40] However, the catalytic properties from copper, in the MOF, were only obtained after modification by transmetalation. Their MOF showed selective gas adsorptions for $CO_2$ over $N_2$, $CH_4$ and $H_2$. In addition, their porous MOF additionally catalysed Knoevenagel condensation reactions using the basic sites and not the Lewis acid sites.[40] Therefore, multifunctional MOFs, combining acidic and basic sites, should undergo systematic investigations

[a]State Key Laboratory of Inorganic Synthesis and Preparative Chemistry, College of Chemistry, Jilin University, Changchun, 130012, China. E-mail: zhugs@jlu.edu.cn; Fax: +86-431-85168331; Tel: +86-431-85168887

[b]Department of Chemistry, University of South Florida, 4202 East Fowler Avenue, Tampa, Florida 33620, USA. E-mail: sqma@usf.edu; Fax: +1-813-974-3203; Tel: +1-813-974-5217

† Electronic supplementary information (ESI) available: PXRD, TGA, FT-IR and so on. CCDC 989570. For ESI and crystallographic data in CIF or other electronic format see DOI: 10.1039/c6ta05098k

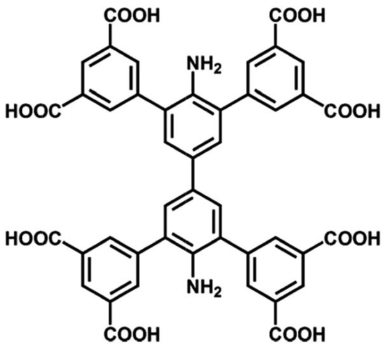


Scheme 1 The ligand $H_8$TBCB.

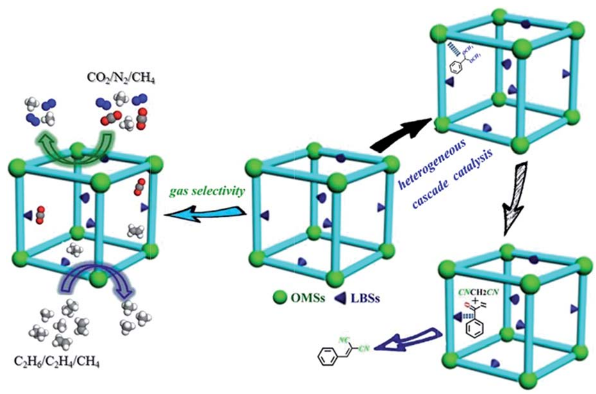


Scheme 2 Schematic illustration of this bifunctional MOF for selective gas adsorption and heterogeneous cascade catalysis.

to determine their built-in properties for gas sorption, separation and catalysis.

The documented studies with amine-functionalization ligands in MOFs for introducing LBSs into the framework,[41–44] have inspired our ligand design of 2,2′,6,6′-tetrakis[3,5-bis-3,5-benzenedicarboxylate] benzidine ($H_8$TBCB) that features two amino functional groups (Scheme 1). Self-assembly of $TBCB^{-8}$ ligand with $Zn^{2+}$ ions under solvothermal conditions afforded a three-dimensional (3D) microporous MOF called JUC-199 having a chemical formula of $[Zn_4(TBCB)\cdot(H_2O)_6]\cdot 5DMAc$ (DMAc = *N*,*N*-dimethylacetamide). By design, the resultant microporous MOF features both OMSs and LBSs, which render it with interesting performances in selective gas adsorption ($CO_2$ over $CH_4$ and $N_2$, and $CH_4$ over $C_2H_6$ and $C_2H_4$) and allow heterogeneous catalysis for the tandem one-pot deacatalization-Knoevenagel condensation reaction (as shown in Scheme 2).

# Experimental section

### Materials and methods

All the chemical reagents were received from commercial sources and used without further purification. HY zeolite ($SiO_2$/$Al_2O_3$ = 30) was purchased from ZEOLYST. $H_8$TBCB synthesis details are found in the ESI.† Powder X-ray-diffraction (PXRD) patterns were acquired on a Scintag X1 diffractometer with Cu-Kα ($\lambda$ = 1.5418 Å) at 50 kV, 40 mA in the range of 4–40° ($2\theta$). Thermogravimetric analyses (TGA) for all measurements were carried on a Perkin-Elmer TGA thermogravimetric analyser under air flow at a heating rate of 10 °C $min^{-1}$ from 30 to 800 °C. Elemental analyses on C, H and N were obtained using a Perkin-Elmer 240 analyzer. Fourier-transform infrared spectra (FT-IR) were performed on a Nicolet Impact 410 FT-IR spectrometer in the 4000–400 $cm^{-1}$ range using KBr pellets. All gas sorption measurements were acquired on the surface area analyser ASAP 2020.

### Synthesis of JUC-199

A mixture of $Zn(NO_3)_2\cdot 6H_2O$ (15 mg, 0.05 mmol), $H_8$TBCB (5 mg, 0.006 mmol), DMAc (3.5 mL), $H_2O$ (1 mL) and two drops of aqueous $HNO_3$ solution (2.0 M) was sealed in a 20 mL capped vessel. The as-synthesized brown crystals can be obtained at 85 °C for 3 days in an oven. The yield is about 62% (based on the ligand). Element analysis (%) calc. for $C_{64}H_{77}O_{27}N_7Zn_4$: C, 46.97; H, 4.71; N, 5.99; found: C, 46.75; H, 4.79; N, 6.07. Selected FT-IR data (KBr pellet, $cm^{-1}$): 2935 (br), 1619 (s), 1412 (s), 1356 (s), 1261 (s), 1186 (s), 1020 (s), 783 (s), 717 (s), 660 (s), 592 (s), 463 (s) (Fig. S1†).

### X-ray structure determination and structure refinement

The single crystal data of JUC-199 was obtained from a Bruker SMART APEX II CCD-based diffractometer with graphite monochromatized Mo-Kα radiation ($\lambda$ = 0.71073 Å) at room temperature. Corrections for incident and diffracted beam absorption effects were applied to the date using the SADBAS program.[45] The crystal structure can be determined by a combination of direct methods and refined by the full matrix least-squares against $F^2$ values using the SHELXTL program.[46] All non-hydrogen atoms were located successfully from Fourier maps and refined by anisotropic thermal parameters. Due

Table 1 Crystal data and structure refinement for JUC-199

| | |
|---|---|
| Compound | JUC-199 |
| Empirical formula | $C_{64}H_{77}O_{27}N_7Zn_4$ |
| Formula weight | 1635.1 |
| Crystal system | Monoclinic |
| Space group | $P2_1/c$ |
| $a$ (Å) | 12.4957(10) |
| $b$ (Å) | 15.3163(14) |
| $c$ (Å) | 24.254(2) |
| $\alpha$ (°) | 90.00 |
| $\beta$ (°) | 102.304(2) |
| $\gamma$ (°) | 90.00 |
| $V$ (Å$^3$) | 4535.3(7) |
| $Z$ | 4 |
| $\rho$ calc. g $cm^{-3}$ | 0.872 |
| $\mu$ ($mm^{-1}$) | 1.090 |
| $N_{ref}$ | 11 550 |
| $F$(000) | 1188.0 |
| $R$(int) | 0.0403 |
| Goodness-of-fit on $F^2$ | 0.988 |
| $R_1$, w$R_2$ [$I > 2\sigma(I)$] | 0.0474, 0.1407 |
| $R_1$, w$R_2$ (all data) | 0.0671, 0.1489 |

to some disordered solvent molecules in JUC-199, their diffraction contributions were removed by using the PLATON/SQUEEZE.[47,48] The guest molecules can be calculated from the results of TGA and elemental analyses. Crystal data of JUC-199 is listed in Table 1 and the selected bond lengths and bond angles are summarized in Table S2.†

## Results and discussion

### Structure

Single-crystal X-ray diffraction study revealed that JUC-199 crystallized in the monoclinic space group $P2_1/c$. The asymmetrical unit of the host framework contains two independent $Zn^{2+}$ ions, one half of the $TBCB^{-8}$ ligand, and three terminal water molecules (Fig. S2†). As shown in Fig. 1a, Zn1 is four-coordinated by four carboxylate oxygen atoms from four different ligands (Zn1–O, 1.9059(19)–1.9478(24) Å), while Zn2 is octahedrally coordinated by three oxygen atoms from three carboxylate oxygen atoms and three oxygen atoms from three terminal water molecules (Zn2–O, 2.0436(19)–2.2034(19) Å). Eight carboxylate groups of each ligand are all connected with $[Zn_2(COO)_4]$ SBUs, six of them adopt a chelating mode and the other two take a monodentating mode. Each $[Zn_2(COO)_4]$ unit is linked with four ligands and each ligand connects eight $[Zn_2(COO)_4]$ SBUs to form a 3D porous framework architecture (Fig. 1b). The solvent accessible volume of JUC-199 is about 64.2% as calculated using PLATON/VOID.[47] Topologically, the binuclear inorganic cluster and the ligand could be simplified as four-connected and eight-connected nodes, respectively. Thus, the network of JUC-199 can be regarded as a (4,8)-net with the topology alb-4,8-$P2_1/c$ (Fig. 1c) and Schläfli symbol is $\{4^{10}\cdot6^{14}\cdot8^4\}\cdot\{4^5\cdot6\}_2$ calculated by TOPOS software.[49–51] The thermogravimetric analyses of JUC-199 (Fig. S3†) showed a weight loss of 33.86% before 200 °C, corresponding to the calculated percentage content of guest and terminal solvent molecules (calculated 34.21%). Powder X-ray diffraction (PXRD) patterns of JUC-199 confirmed the phase purity of the bulk crystalline material (Fig. S4†). In addition, JUC-199 exhibited good stability in air and water vapour, which was confirmed by the PXRD patterns (Fig. S5†).

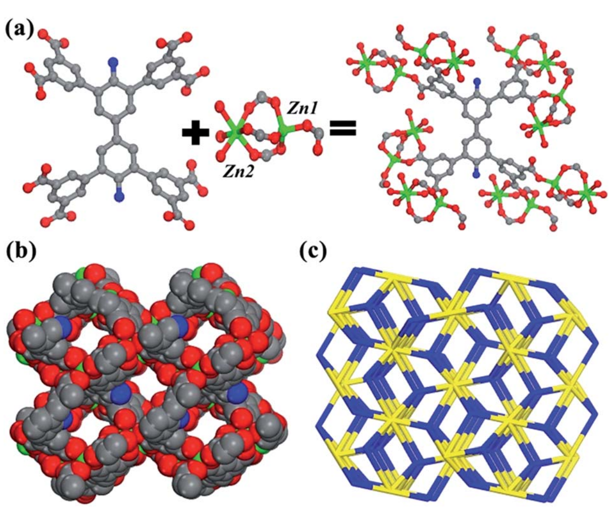


Fig. 1 (a) The ligand and the inorganic cluster in JUC-199; (b) the spacefill pattern of 3D framework (Zn: green; C: gray; O: red; N: blue); (c) the simplified topology structure. The hydrogen atoms are omitted for clarity.

### Gas sorption properties

To assess the permanent porosity of JUC-199, the freshly prepared samples were soaked in dry methanol, which was further desolvated using a supercritical $CO_2$ dryer.[52] The $N_2$ sorption isotherms of the activated sample at 77 K (Fig. 2) revealed a completely reversible type-I behaviour, a characteristic of microporous materials. Based on the $N_2$ adsorption data, the Brunauer–Emmett–Teller (BET) surface area and Langmuir surface area of JUC-199 were calculated to be 821 $m^2\ g^{-1}$ and 953 $m^2\ g^{-1}$, respectively with a corresponding pore volume of 0.36 $cm^3\ g^{-1}$. As shown in Fig. S6,† the pore size distribution ranged from 7.79 to 10.29 Å (as determined using the Horvath–Kawazoe method). The surface area is smaller than the theoretically calculated accessible surface area of 1171 $m^2\ g^{-1}$ (Fig. S7†), which is mainly attributed to the partial pore blockage or collapse of the host framework during activation. As shown in Fig. S4,† the PXRD pattern of the activated sample indicated that the main original skeleton was still retained after activation. However, some extra peaks appeared in the PXRD patterns because of the partial collapse of the host framework after guest removal.

We further investigated the sorption behaviours of activated JUC-199 for some other small gases. The adsorption enthalpy ($Q_{st}$) was calculated from the adsorption isotherms at 273 and 298 K using the virial method. The $CO_2$ adsorption capacity was observed to be 55 $cm^3\ g^{-1}$ (2.46 mmol $g^{-1}$) and 40 $cm^3\ g^{-1}$ (1.78 mmol $g^{-1}$) at 273 K and 298 K respectively under 1 atm pressure (Fig. 3a). The $Q_{st}$ of $CO_2$ was 29 kJ $mol^{-1}$ at zero loading (Fig. 3f and S8†) which was higher than that of most "benchmark MOFs", such as CuBTTri (21 kJ $mol^{-1}$),[53] MOF-5 (17 kJ $mol^{-1}$),[54] UMCM-1 (12 kJ $mol^{-1}$),[55] and NOTT-140 (25 kJ $mol^{-1}$),[56] and is comparable to that of MIL-53(Cr) (32 kJ $mol^{-1}$),[57] HKUST-1 (hydrated) (30 kJ $mol^{-1}$)[58] and MAF-2 (27 kJ $mol^{-1}$).[59] JUC-199 high adsorption enthalpy is mainly due to the strong interactions of $CO_2$ with both exposed Zn sites and amino functional groups.

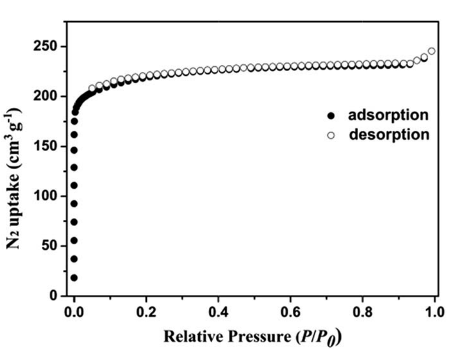


Fig. 2 $N_2$ sorption isotherms of the activated sample at 77 K (solid symbols: adsorption and open symbols: desorption).

 

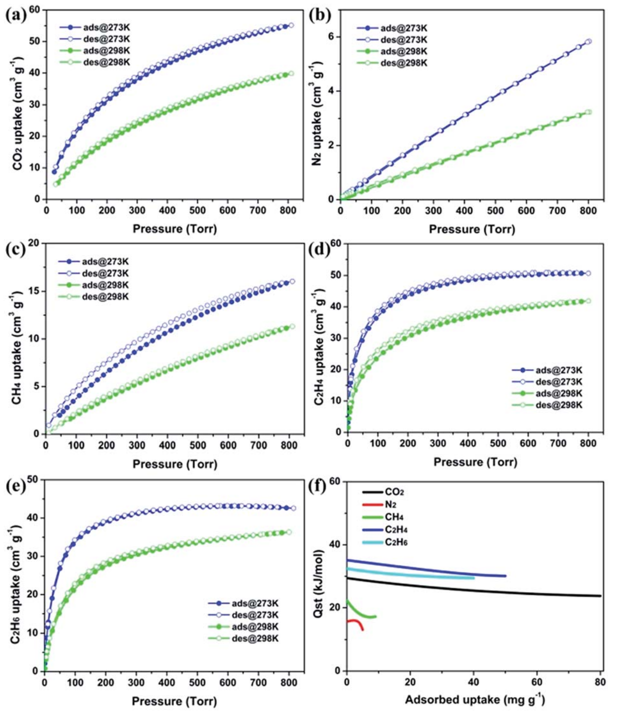


Fig. 3 Gas sorption isotherms of $CO_2$ (a), $N_2$ (b), $CH_4$ (c), $C_2H_4$ (d) and $C_2H_6$ (e) at 273 K and 298 K; (f) the $Q_{st}$ of these gases for JUC-199.

In addition, the sorption isotherms of $N_2$ and $CH_4$ were also measured at 273 K and 298 K under 1 atm pressure (Fig. 3b and c). The adsorption capacities for $N_2$ are 6.3 $cm^3$ $g^{-1}$ (0.28 mmol $g^{-1}$) and 3.5 $cm^3$ $g^{-1}$ (0.16 mmol $g^{-1}$) at 273 K and 298 K respectively; and the values for $CH_4$ are 16 $cm^3$ $g^{-1}$ (0.72 mmol $g^{-1}$) and 11 $cm^3$ $g^{-1}$ (0.51 mmol $g^{-1}$) at 273 K and 298 K respectively. At zero loading, the $Q_{st}$ of $N_2$ and $CH_4$ are 16 and 22 kJ $mol^{-1}$, respectively (Fig. 3f, S9 and S10†). In order to estimate the practical separation ability for $CO_2$, theoretical gas mixtures of $CO_2/N_2$ and $CO_2/CH_4$ are evaluated by the IAST model,[60] a method used to determine binary mixture adsorption from experimental single-component isotherms. The dual-site Langmuir–Frendlich equation was employed to fit the data (Fig. 4a) with excellent correlation coefficients. The estimated selectivity data were obtained from a function of pressure at a general feed composition of landfill gas (50/50, m/m) at 298 K under 101 kPa (Fig. 4b). At 298 K and 101 kPa, the selectivity values for $CO_2/CH_4$ and $CO_2/N_2$ are 9 and 30, respectively, which are significantly higher than those of many reported MOFs under the same conditions.[61–63]

Additionally, hydrocarbons ethylene and ethane were measured at 273 and 298 K under 1 atm pressure (Fig. 3d and e). The uptake capacities of $C_2H_4$ are 51 $cm^3$ $g^{-1}$ (2.26 mmol $g^{-1}$) and 42 $cm^3$ $g^{-1}$ (1.87 mmol $g^{-1}$) at 273 and 298 K respectively; and the values for $C_2H_6$ are 42 $cm^3$ $g^{-1}$ (1.90 mmol $g^{-1}$) and 36 $cm^3$ $g^{-1}$ (1.62 mmol $g^{-1}$) at 273 and 298 K respectively. The $Q_{st}$ values at zero coverage are 35 and 32 kJ $mol^{-1}$ for $C_2H_4$ and $C_2H_6$ respectively (Fig. 3f, S11 and S12†). The dual-site Langmuir–Frendlich equation was applied to fit the experimental data (Fig. 4c). As shown in Fig. 4d, the estimated selectivity data

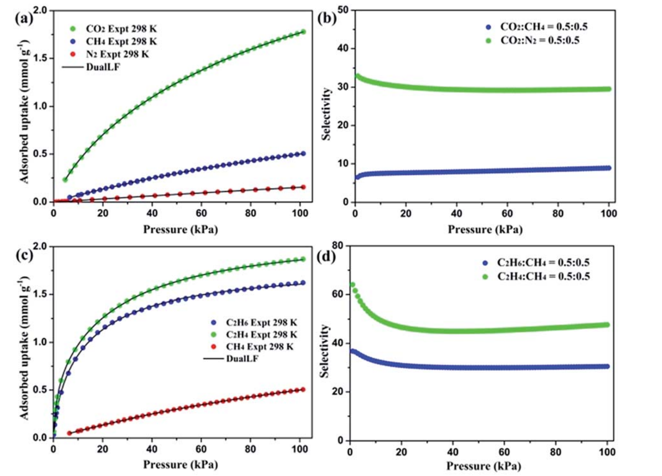


Fig. 4 Gas sorption isotherms of $CO_2$, $N_2$, $CH_4$, $C_2H_4$ and $C_2H_6$ along with the dual-site Langmuir–Freundlich (DSLF) fits (a and c); gas mixture adsorption selectivity are predicted by IAST for JUC-199 at 298 K and 101 kPa (b and d).

are obtained from a function of pressure at a general feed composition of landfill gas (50/50, m/m). At 298 K and 101 kPa, the $C_2H_6/CH_4$ adsorption selectivity of 37 is higher than many reported MOFs, such as Mg–MOF-74 (11.5), NOTT-101 (12) and FIR-7a (14.6).[64,65] The selectivity value of 64 for $C_2H_4/CH_4$, is also much higher than many reported MOFs.[66,67] As shown in Fig. 3f, the $Q_{st}$ trends of $C_2H_6$, $C_2H_4$, $CH_4$, and $CO_2$ all steadily decreases with increasing gas adsorption uptake because the interactions between host and guest molecules reaches a maximum when all the exposed Zn sites and amino functional groups become saturated by guest initially and then guest–guest interactions occur. However, the $Q_{st}$ trend for $N_2$ differs from the other gas molecules because there is weak interactions with the host framework. In addition, these results suggested that JUC-199 could be an efficient microporous material not only for efficiently capture and separation of $CO_2$ but also for purification of $CH_4$ from natural gas and biogas.

## Catalytic property

Up to now, only a few MOFs have been reported for the acid–base one-pot reaction with high yields.[68–74] Given the existence of both OMSs and LBSs in the framework, JUC-199 was examined as a bifunctional acid–base catalyst for one-pot cascade reaction. The acid-catalyzed acetal hydrolysis and the subsequent base-catalyzed Knoevenagel condensation were chosen as the model reaction (Table 2). In a typical experiment, the catalytic reactions were carried out in a 20 mL glass reactor vial. A mixture of substrate (1 mmol), malononitrile (1.2 mmol), 1,4-dioxane (4 mL) with 100 mg of the catalyst was stirred at 363 K for 4 hours. The products were monitored by GC-MS equipped with a DB-5HT column. JUC-199 effectively catalysed benzaldehyde dimethylacetal (1) into benzylidenemalononitrile (3) in almost quantitative yield in 4 h (Table 2, entry 1). In contrast, HY zeolite catalysed the first reaction step from the acidic catalyst (entry 2). MgO, a basic solid catalyst, showed little

Table 2 One-pot deacetalization–Knoevenagel condensation reaction[a]

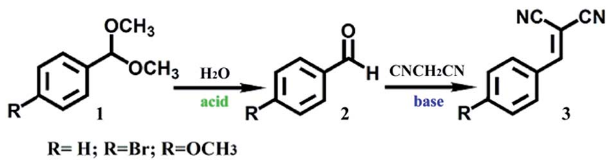


| Entry | R | Catalyst | Conv. 1 [%][e] | Yield 2 [%][e] | Yield 3 [%][e] |
|---|---|---|---|---|---|
| 1 | H | JUC-199 | ≥99 | Trace | ≥99 |
| 2 | H | HY zeolite | ≥99 | 93 | 7 |
| 3 | H | MgO | 8 | 3 | 5 |
| 4 | H | HY zeolite + MgO[b] | 93 | 58 | 35 |
| 5 | H | HCl[c] | ≥99 | 96 | 4 |
| 6 | H | TEA[c] | Trace | Trace | Trace |
| 7 | H | HCl + TEA[d] | Trace | Trace | Trace |
| 8 | Br | JUC-199 | 94 | Trace | 94 |
| 9 | $OCH_3$ | JUC-199 | 92 | Trace | 92 |
| 10 | H | No catalyst | Trace | Trace | Trace |
| 11 | H | 3rd recycle | ≥99 | Trace | ≥99 |

[a] Reaction conditions: substrate (1 mmol), malononitrile (1.2 mmol), 1,4-dioxane (4 mL), catalyst (100 mg), 363 K, 4 h. [b] The mixture of HY zeolite (50 mg) and MgO (50 mg) was employed as the catalyst. [c] 0.1 mmol of HCl or triethylamine (TEA) was used. [d] The mixture of HCl (0.05 mmol) and TEA (0.05 mmol) was employed as the catalyst. [e] The yields were determined by GC-MS.



reactivity (entry 3). In addition, when a mixture of HY zeolite and MgO was employed, the reaction conversion was lower than that of JUC-199 (entry 4). On the other hand, the homogeneous catalysts such as HCl and triethylamine (TEA) were applied for the one-pot reaction. The acid catalyst (HCl) can only efficiently catalyse the quantitative deprotonation of 1 to 2 (entry 5). On the other hand, TEA as a basic catalyst support this reactions even after 4 h (entry 6). When the mixture of HCl (0.05 mmol) and TEA (0.05 mmol) was employed as the catalyst, the reaction hardly occurred (entry 7). It is well known that acid and base catalysts can easily neutralise each other in the homogeneous systems, thus leading to the deactivation of catalysts. When –Br or –OMe groups were introduced into the phenyl ring, the corresponding deacetalization–Knoevenagel condensation products were about 94% (entry 8) and 92% (entry 9) under the same conditions. This phenomenon may be primarily ascribed to the restricted diffusion of large-sized substitute molecules into the framework. In addition, it was also observed that the reaction can't occur in the absence of a catalyst (entry 10). The results clearly demonstrate that JUC-199 can serve as an efficient bifunctional acid–base catalyst for one-pot deacetalization–Knoevenagel condensation reaction.

Furthermore, no detectable leaching of $Zn^{2+}$ ions were observed in the reaction solution after removal of JUC-199 as analysed using inductively coupled plasma (ICP), which confirmed the heterogeneous nature of the catalyst. It was also easy to separate and reuse the catalyst after each reaction. In fact, JUC-199 can be recycled by filtration and washed fresh 1,4-dioxane to prepare it for a following reaction. As shown in entry 11, JUC-199 can be reused for at least three cycles without any loss of activity, and the retention of its framework integrity after catalysis has been verified by PXRD studies (Fig. S13†).

## Conclusion

In summary, we have successfully designed and synthesized a microporous MOF with a high density of OMSs and LBSs. It exhibits high adsorption selectivity for $CO_2$ over $CH_4$ and $N_2$, and $CH_4$ over $C_2H_6$ and $C_2H_4$. In addition, it can serve as a cooperative catalyst for a one-pot deacetalization–Knoevenagel reaction. We anticipate that it can offer a common avenue to obtain multi-functional MOFs. Further work to employ this strategy is ongoing in our research laboratories.

## Acknowledgements

We are grateful for the financial support of National Basic Research Program of China (973 Program, grant no. 2012CB821700 and 2014CB931804), Major International (Regional) Joint Research project of NSFC (grant no. 21120102034), NSFC Project (grant no. 21531003), NSF (DMR-1352065) and USF for financial support of this work.

## Notes and references

1 E. D. Bloch, L. J. Murray, W. L. Queen, S. Chavan, S. N. Maximoff, J. P. Bigi, R. Krishna, V. K. Peterson, F. Grandjean, G. J. Long, B. Smit, S. Bordiga, C. M. Brown and J. R. Long, *J. Am. Chem. Soc.*, 2011, **133**, 14814.
2 Z. Zhang, Z. Z. Yao, S. Xiang and B. Chen, *Energy Environ. Sci.*, 2014, **7**, 2868.
3 S. Xiang, Y. He, Z. Zhang, H. Wu, W. Zhou, R. Krishna and B. Chen, *Nat. Commun.*, 2012, **3**, 954.

 

4 J. D. Shakun, P. U. Clark, F. He, S. A. Marcott, A. C. Mix, Z. Y. Liu, B. Otto-Bliesner, A. Schmittner and E. Bard, *Nature*, 2012, **484**, 49.
5 O. Shekhah, Y. Belmabkhout, K. Adil, P. M. Bhatt, A. J. Cairns and M. Eddaoudi, *Chem. Commun.*, 2015, **51**, 13595.
6 H. He, Y. Song, C. Zhang, F. Sun, R. Yuan, Z. Bian, L. Gao and G. Zhu, *Chem. Commun.*, 2015, **51**, 9463.
7 S. D. Burd, S. Ma, J. A. Perman, B. J. Sikora, R. Q. Snurr, P. K. Thallaapally, J. Tian, L. Wojtas and M. J. Zaworotko, *J. Am. Chem. Soc.*, 2012, **134**, 3663.
8 R. S. Haszeldine, *Science*, 2009, **325**, 1647.
9 A. U. Czaja, N. Trukhanb and U. Muller, *Chem. Soc. Rev.*, 2009, **38**, 1284.
10 Y. He, W. Zhou, G. Qian and B. Chen, *Chem. Soc. Rev.*, 2014, **43**, 5657.
11 J. M. Lee, Y. Na, H. Han and S. Chang, *Chem. Soc. Rev.*, 2004, **33**, 302.
12 J. C. Wasilke, S. J. Obrey, R. T. Baker and G. C. Bazan, *Chem. Rev.*, 2005, **105**, 1001.
13 B. M. Trost, *Science*, 1991, **254**, 1471.
14 J. Jiang and O. M. Yaghi, *Chem. Rev.*, 2015, **115**, 6966.
15 H.-C. Zhou and S. Kitagawa, *Chem. Soc. Rev.*, 2014, **43**, 5415.
16 S. Qiu, M. Xue and G. Zhu, *Chem. Soc. Rev.*, 2014, **43**, 6116.
17 C. He, D. Liu and W. Lin, *Chem. Rev.*, 2015, **115**, 11079.
18 C. K. Brozek and M. Dincǎ, *Chem. Soc. Rev.*, 2014, **43**, 5456.
19 H.-C. Zhou, J. R. Long and O. M. Yaghi, *Chem. Rev.*, 2012, **112**, 673.
20 B. Li, M. Chrzanowski, Y. Zhang and S. Ma, *Coord. Chem. Rev.*, 2016, **307**, 106.
21 W.-Y. Gao, M. Chrzanowski and S. Ma, *Chem. Soc. Rev.*, 2014, **43**, 5841.
22 Y. Liu, S.-Y. Moon, J. T. Hupp and O. K. Farha, *ACS Nano*, 2015, **9**, 12358.
23 B. Li, K. Leng, Y. Zhang, J. Dynes, J. Wang, Y. Hu, D. Ma, Z. Shi, L. Zhu, D. Zhang, Y. Sun, M. Chrzanowski and S. Ma, *J. Am. Chem. Soc.*, 2015, **137**, 4243.
24 D. Chen, H. Xing, C. Wang and Z. Su, *J. Mater. Chem. A*, 2016, **4**, 2657.
25 Y. Zhang, B. Li, R. Krishna, Z. Wu, D. Ma, Z. Shi, T. Pham, K. Forrest, B. Space and S. Ma, *Chem. Commun.*, 2015, **51**, 2714.
26 Q.-G. Zhai, X. Bu, X. Zhao, C. Mao, F. Bu, X. Chen and P. Feng, *Cryst. Growth Des.*, 2016, **16**, 1261.
27 F. Wang, H.-R. Fu, Y. Kang and J. Zhang, *Chem. Commun.*, 2014, **50**, 12065.
28 Z. Hu, W. P. Lustig, J. Zhang, C. Zheng, H. Wang, S. J. Teat, Q. Gong, N. D. Rudd and J. Li, *J. Am. Chem. Soc.*, 2015, **137**, 16209.
29 H. He, Y. Song, F. Sun, N. Zhao and G. Zhu, *Cryst. Growth Des.*, 2015, **15**, 2033.
30 X. Liu, H. Lin, Z. Xiao, W. Fan, A. Huang, R. Wang, L. Zhang and D. Sun, *Dalton Trans.*, 2016, **45**, 3743.
31 H. He, Y. Song, F. Sun, Z. Bian, L. Gao and G. Zhu, *J. Mater. Chem. A*, 2015, **3**, 16598.
32 H. He, F. Sun, J. Jia, Z. Bian, N. Zhao, X. Qiu, L. Gao and G. Zhu, *Cryst. Growth Des.*, 2014, **14**, 4258.
33 H. Su, F. Sun, J. Jia, H. He, A. Wang and G. Zhu, *Chem. Commun.*, 2015, **51**, 5774.
34 P. Horcajada, T. Chalati, C. Serre, B. Gillet, C. Sebrie, T. B. J. F. Eubank, A. Heurtaux, P. Clayette, C. Kreuz, J.-S. Chang, Y. K. Hwang, V. Marsaud, P.-N. Bories, L. Cynober, S. Gil, G. Ferey, P. Couvreur and R. Gref, *Nat. Mater.*, 2010, **9**, 172.
35 P. P. Bag, D. Wang, Z. Chen and R. Cao, *Chem. Commun.*, 2016, **52**, 3669.
36 H. Zhang, P. Lin, X. Shan, F. Du, Q. Li and S. Du, *Chem. Commun.*, 2013, **49**, 2231.
37 H. He, F. Sun, T. Borjigin, N. Zhao and G. Zhu, *Dalton Trans.*, 2014, **43**, 3716.
38 W. Xie, W.-W. He, D.-Y. Du, S.-L. Li, J.-S. Qin, Z.-M. Su, C.-Y. Sun and Y.-Q. Lan, *Chem. Commun.*, 2016, **52**, 3288.
39 Y. He, B. Li, M. O'Keeffe and B. Chen, *Chem. Soc. Rev.*, 2014, **43**, 5618.
40 T. K. Pal, D. De, S. Neogi, P. Pachfule, S. Senthilkumar, Q. Xu and P. K. Bharadwaj, *Chem.–Eur. J.*, 2015, **21**, 19064.
41 T.-L. Hu, H. Wang, B. Li, R. Krishna, H. Wu, W. Zhou, Y. Zhao, Y. Han, X. Wang, W. Zhu, Z. Yao, S. Xiang and B. Chen, *Nat. Commun.*, 2015, **6**, 7328.
42 Y. Lin, C. Kong and L. Chen, *RSC Adv.*, 2012, **2**, 6417.
43 D.-M. Chen, N. Xu, X.-H. Qiu and P. Cheng, *Cryst. Growth Des.*, 2015, **15**, 961.
44 Y. Lin, C. Kong and L. Chen, *RSC Adv.*, 2016, **6**, 32598.
45 G. M. Sheldrick, *SADABS, Program for Empirical Absorption Correction for Area Detector Data*, University of Gottingen, Gottingen, Germany, 1996.
46 G. M. Sheldrick, *SHELXTL Version 5.1 Software Reference Manual*, Bruker AXS. Inc., Madison, WI, 1997.
47 A. L. Spek, *J. Appl. Crystallogr.*, 2003, **36**, 7.
48 A. L. Spek, *PLATON, A multipurpose crystallographic tool*, Utrecht University, The Netherlands, 2001.
49 V. A. Blatov and A. P. Shevchenko, *TOPOS-Version 4.0 Professional (beta evaluation)*, Samara State University, Samara, Russia, 2006.
50 V. A. Blatov, A. P. Shevchenko and V. N. Serezhkin, *J. Appl. Crystallogr.*, 2000, **33**, 1193.
51 http://www.topos.ssu.samara.ru.
52 A. P. Nelson, O. K. Farha, K. L. Mulfort and J. T. Hupp, *J. Am. Chem. Soc.*, 2009, **131**, 458.
53 A. D. Demessence, M. D. Alessandro, M. L. Foo and J. R. Long, *J. Am. Chem. Soc.*, 2009, **131**, 8784.
54 J.-S. Choi, W.-J. Son, J. Kim and W.-S. Ahn, *Microporous Mesoporous Mater.*, 2008, **116**, 727.
55 B. Mu, P. M. Walton and K. S. Walton, *J. Phys. Chem. C*, 2010, **114**, 6464.
56 C. Tan, S. Yang, N. R. Champness, X. Lin, A. J. Blake, W. Lewis and M. Schröder, *Chem. Commun.*, 2011, **47**, 4487.
57 S. Bourrelly, P. L. Llewellyn, C. Serre, F. Millange, T. Loiseau and G. Férey, *J. Am. Chem. Soc.*, 2005, **127**, 13519.
58 Z. Liang, M. Marshall and A. L. Chaffee, *Energy Procedia*, 2009, **1**, 1265.
59 J.-P. Zhang and X.-M. Chen, *J. Am. Chem. Soc.*, 2009, **131**, 5516.
60 A. L. Myers and J. M. Prausnitz, *AIChE J.*, 1965, **11**, 121.

61 M.-H. Choi, H. J. Park, D. H. Hong and M. P. Suh, *Chem.–Eur. J.*, 2013, **19**, 17432.
62 A. Phan, C. J. Doonan, F. J. Uribe-Romo, C. B. Knobler, M. O'Keeffe and O. M. Yaghi, *Acc. Chem. Res.*, 2010, **43**, 58.
63 S. Yao, D. Wang, Y. Cao, G. Li, Q. Huo and Y. Liu, *J. Mater. Chem. A*, 2015, **3**, 16627.
64 X.-L. Si, C.-L. Jiao, F. Li, J. Zhang, S. Wang, S. Wang, S. Liu, Z.-B. Li, L.-X. Sun, F. Xu, Z. Gabelica and C. Schick, *Energy Environ. Sci.*, 2011, **4**, 4522.
65 Y.-P. He, Y.-X. Tan and J. Zhang, *Chem. Commun.*, 2013, **49**, 11323.
66 K. Liu, B. Li, Y. Li, X. Li, F. Yang, G. Zeng, Y. Peng, Z. Zhang, G. Li, Z. Shi, S. Feng and D. Song, *Chem. Commun.*, 2014, **50**, 5031.
67 Q.-R. Ding and F. Wang, *Dalton Trans.*, 2016, **45**, 7004.
68 J. Park, J.-R. Li, Y.-P. Chen, J. Yu, A. A. Yakovenko, Z. U. Wang, L.-B. Sun, P. B. Balbuena and H.-C. Zhou, *Chem. Commun.*, 2012, **48**, 9995.
69 Y. Pan, B. Yuan, Y. Li and D. He, *Chem. Commun.*, 2010, **46**, 2280.
70 F. Song, C. Wang and W. Lin, *Chem. Commun.*, 2011, **47**, 8256.
71 B. Li, Y. Zhang, D. Ma, L. Li, G. Li, Z. Shi and S. Feng, *Chem. Commun.*, 2012, **48**, 6151.
72 T. Toyao, M. Fujiwaki, Y. Horiuchi and M. Matsuoka, *RSC Adv.*, 2013, **3**, 31582.
73 P. V. Dau and S. M. Cohen, *Inorg. Chem.*, 2015, **54**, 3134.
74 Y.-R. Lee, Y.-M. Chung and W.-S. Ahnss, *RSC Adv.*, 2014, **4**, 23064.


 